J Mater Sci: Mater Electron **(2024) 35:302**

Investigation of the influence of Al layer and total film thicknesses on structural and related magnetic properties in sputtered Ni/Al multilayer thin films

Nadir Kaplan[1], Hilal Kuru[1], and Hakan Köçkar[1,*]

[1] *Department of Physics, Faculty of Science and Literature, University of Balikesir, Cagis, 10145 Balikesir, Turkey*

Received: 12 December 2023
Accepted: 12 January 2024
Published online:
6 February 2024

© The Author(s), 2024

ABSTRACT

The effects of parameters of Al layer thickness and total film thickness on the structural and related magnetic properties of Ni/Al multilayer films were investigated. The films were deposited by a dual sputtering. The Ni content decreased gradually while the Al content increased as the Al layer thickness increased. It was also observed that the total film thickness had little effect on the film content. All films have a face-centred cubic structure. And, the surface morphology of Ni/Al films is more uniform and homogeneous than the surface of Ni film. For magnetic analysis, the properties were strongly changed with the parameters. The saturation magnetisation, M_s of Ni film was obtained as 572 emu/cm^3 while the M_s of the Ni/Al films decreased from 441 to 298 emu/cm^3 with increasing Al content in the films caused by the Al layer thickness. And, the increase of total film thickness resulted in a decrease of M_s value. While the coercivity, H_c value of the Ni film was 90 Oe, H_c of Ni/Al films was decreased to ~ 39 Oe with the formation of multilayer structure. Ni/Al multilayers were obtained magnetically softer than the Ni film. The M_s and H_c values were significantly affected by the variation of the film content and crystal structure caused by the changes in deposition parameters. Therefore, this is a fundamental step for Ni/Al multilayers to improve the properties of these films for their potential applications in microelectronic devices.

1 Introduction

The high saturation magnetization and low coercivity of soft magnetic multilayers with nanometer layer thickness make them promising candidates for use in electromagnetic devices as magnetoresistive sensors and storage devices [1–3]. In recent years, with the increasing need to reduce device size, research on the production and characterization of new soft magnetic multilayers with nanometer layer thicknesses exhibiting unusual magnetic properties has accelerated. Production of nanolayered magnetic multilayers can be done by several methods such as sputtering, vapor deposition and electrodeposition [4–7]. Among the techniques, DC magnetron sputtering is one of the most widely used methods in multilayer

Address correspondence to E-mail: hkockar@balikesir.edu.tr

E-mail Addresses: nadirkaplan@baun.edu.tr; htopcu@balikesir.edu.tr

https://doi.org/10.1007/s10854-024-12008-6

manufacturing. The technique offers more uniform and high quality deposition surface, quick growth, composition control and a clean environment free of toxic chemicals [8]. The microstructure and physical properties of multilayers used for various purposes in different technological devices can be controlled by adjusting process parameters such as layer thicknesses, total film thickness, deposition rate, substrate type and temperature [4, 8–11]. In particular, the layer thickness is an effective parameter in the sputtering process [1, 12].

It is known that multilayers consisting of Ni layers are frequently investigated by many researchers [13–17]. The main reason for this interest is that Ni containing multilayers have a wide field of applications in various advanced devices due to their excellent performance in magnetic, mechanical and electrical properties. Among the Ni containing multilayers, focusing on Ni/Al multilayers has many advantages, as their applications in technology are rapidly expanding and they can also exhibit attractive magnetic properties. Besides, Ni/Al is a reactive multilayer thin film and has been studied in several researches in joining applications as local heat sources for soldering and brazing due to their self-propagating nature studied the structural changes of Ni/Al multilayers with different modulation periods at increasing temperatures [13]. In the study, it was obtained that the structural evolution depends on the multilayer period and were affected by overall chemical compositions. In addition, the sequence of phase formation and the microstructural evolution of Ni/Al multilayer thin films during the heat treatments were investigated by Simones et al. [14]. Besides, the effects of the Al/Ni molar ratio on the reaction are studied by varying the thicknesses of the Al/Ni bilayers by Kuk et al. [15]. Recently, the study [16] demonstrated the self-propagating reaction and adhesion between the Ni/Al multilayers and silicon substrate. When considering the studies done by now, researches on the Ni/Al multilayers have focused on structural evolution and thermal effects. And there is only one study in the literature investigating the structural and magnetic properties of Ni/Al multilayers with the effect of Ni layer thickness [17]. To our knowledge, there is no investigation on dependency of Al layer thickness and total film thickness on the properties of sputtered Ni/Al multilayer films. Therefore, the purpose of this study is to fill in the gap of the field and investigate the influence of Al layer thickness and total film thickness on the microstructural and related magnetic properties of Ni/Al multilayer films. Increasing Al layer thickness from 0 to 17.5 nm, the differences obtained from the compositional and structural analysis of the films consequently leads to significant changes in their magnetic properties. The saturation magnetisation of the Ni/Al multilayers decreased with the increase of Al layer thickness and total film thickness. It is seen that the structural and related magnetic properties of the Ni/Al multilayers are sensitive to production parameters and may have the potential applications in microelectronic devices.

2 Experimental

The Ni/Al multilayers were grown on polymer substrates (commercial acrylic acetate sheet) at room temperature by a dual DC magnetron sputtering (MANTIS, Q-Prep 500, UK). The high-purity metallic Nickel and Aluminum (Kurt J. Lesker Company, 99.99%) approximately 2 mm thick and 50.8 mm in diameter were used as targets. Before the growth process of the multilayers, the targets and the substrates were washed with pure water and then with isopropyl alcohol in an ultrasonic bath (Isolab, 621.05.006, Germany) for 10 min. After the cleaning process, they were dried spontaneously at room conditions. Then, the targets placed separately on the DC magnetrons in the vacuum chamber of the system. All films were sputtered at a pressure of around 4.50×10^{-3} mbar. During the sputtering process, the layer thicknesses were monitored by thickness monitor (Sycon, STM-100/MF, US).

In the first series, in order to study the effect of Al layer thickness on the structural and magnetic properties of Ni/Al multilayer films, while the Al layer thicknesses were changed as 0, 5.0, 10.0 and 17.5 nm, the Ni layer thickness and the total film thickness were kept constant at 20 and 150 nm, respectively. A schematic demonstration of the multilayer structure as $N[t_{Ni}(20\ nm)/t_{Al}(nm)]$ is shown in Fig. 1. The bilayer number "N" coefficients were taken to be 6, 5, and 4, respectively, to give a total film thickness of 150.0 nm. In the second series, in order to study the effect of total film thickness, the Ni layer thickness and Al layer thickness was kept constant at 20 and 5.0 nm, respectively, and the total film thickness was varied between 100 and 200 nm at 25 nm intervals. Therefore, the "N" coefficients were taken to be 4, 5, 6, 7 and 8 to obtain $N[t_{Ni}(20\ nm)/t_{Al}(5\ nm)]$ multilayers. The deposition rates were kept constant at 0.10 nm/s for Ni and at

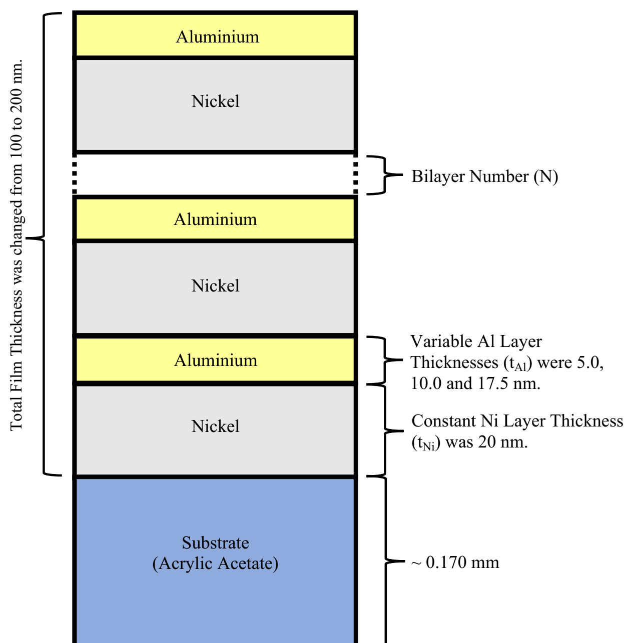

Fig. 1 The schematic cross-section of the Ni/Al multilayer thin film structure

0.03 nm/s for Al, respectively. All films were deposited at the rotation speed of 20 ± 0.2 rpm.

Atomic content analyses of the films were carried out by using an energy dispersive X-ray spectroscopy (EDX, EDAX Element, AMETEK, USA). And, the crystal structure of the films was studied by using an X-ray diffractometer (Bruker, Advance with Davinci Design for XRD^2, U.K.) with an X-ray detector (LYNXEYE XE). The grazing incidence X-ray diffraction (GIXRD) patterns of the films were obtained by varying the 2θ angle between 30° and 80° in steps of 0.02° with Cu-Kα radiation (λ = 0.154056 nm) at an angle of incidence of 5° to the film surfaces. Also, the surface morphologies of the films were observed by using a scanning electron microscope (SEM; Hitachi, SU5000, Japan). For magnetic measurements, the hysteresis loops of the multilayer films were obtained by using a vibrating sample magnetometer (VSM; ADE TECHNOLOGIES DMS-EV9, USA) within a magnetic field of ± 20 kOe at room temperature. The magnetisation values in hysteresis loops were obtained from magnetic moments (VSM) divided by whole films volumes (calculated). The magnetic measurement accuracy of the magnetometer was 1×10^{-6} emu. In addition, the magnetic loops of the films were plotted in a narrower range to provide more detailed figures. For the magnetic measurement, the multilayer films were cut into circles with a diameter of 6 mm to avoid shape-anisotropy.

3 Results and discussion

The atomic content, crystalline structure and magnetic data of the Ni/Al multilayer films produced with different Al layer and total film thicknesses are given in Table 1. Compositional analysis with EDX shows that Ni film contains 99.8 at.% Ni while the films with Al layer thicknesses of 5.0, 10.0 and 17.5 nm contain 64.0, 50.6 and 49.6 at.% Ni and 35.8, 49.2, 50.2 at.%

Table 1 Compositional, crystalline structure and magnetic data of the sputtered Ni/Al films produced at different Al layer and total film thicknesses

Thickness (nm)		*Composition analysis (EDX)		Crystalline properties (GIXRD)			Magnetic properties (VSM)	
Al layer	Total film	Ni (at.%)	Al (at.%)	t (nm)	d (nm)	a (nm)	M_S (emu/cm^3)	H_C (Oe)
0	150	99.8	0.0	7	0.2025	0.3508	572	90
5.0		64.0	35.8	9	0.2363	0.4092	441	38
10.0		50.6	49.2	10	0.2363	0.4092	383	40
17.5		49.6	50.2	10	0.2361	0.4090	298	39
5.0	**100**	60.4	39.4	8	0.2043	0.4086	450	52
	125	–	–	–	–	–	446	46
	150	57.0	42.8	7	0.2040	0.4081	441	38
	175	–	–	–	–	–	431	47
	200	55.5	44.3	7	0.2041	0.4082	427	45

Bold values are significant

*Each film contained up to 0.2% of other impurities such as O, H and C

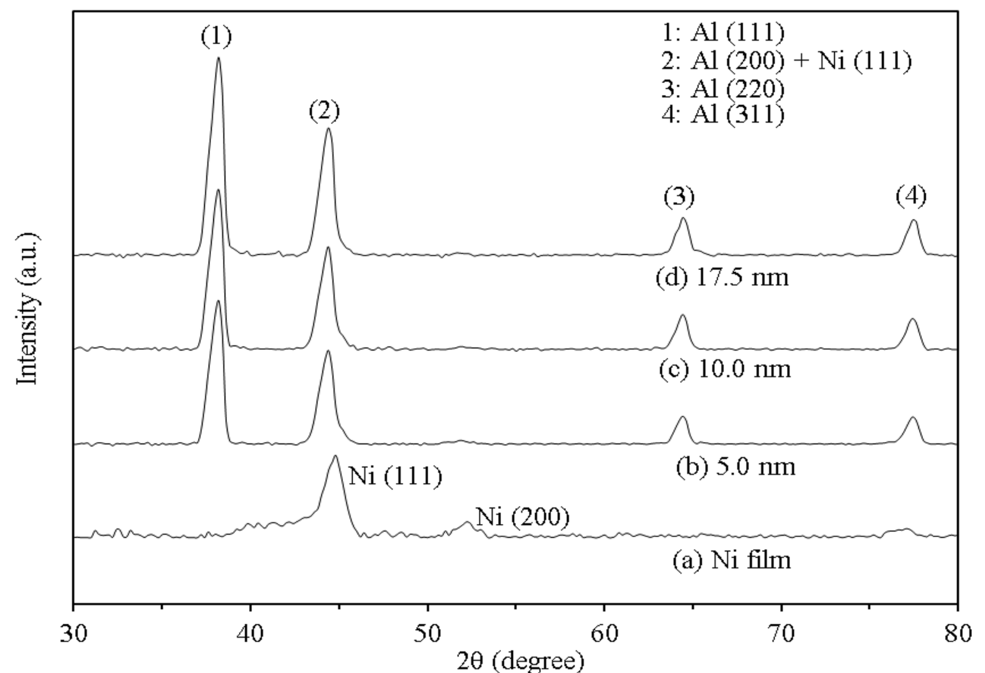

Fig. 2 The GIXRD patterns of the Ni film and Ni/Al multilayers produced with different Al layer thicknesses

Al, respectively. All of the films contain 0.2% impurity atoms such as O, H, and C according to EDX analysis. As can be seen, the increase in Al layer thickness caused a gradual decrease in Ni content and an increase in Al content. The observed variation in Ni and Al content is mainly due to variation of Al layer thickness. For the films produced with different total film thicknesses, the Ni and Al contents obtained for the 100 nm thickness of Ni/Al multilayer were determined as 60.4 and 39.4 at.%, respectively. When the total film thickness was raised to 150 nm, the Ni and Al contents in the multilayer were determined as 57.0 and 42.8 at.%, respectively. In the elemental analysis of the multilayer with a thickness of 200 nm, it was determined that the film contain 55.5 at.% Ni and 44.3 at.% Al. And, a slight change in the film content is observed as the total film thickness changes.

Figures 2 and 3 show the GIXRD patterns of Ni/Al multilayer thin films sputtered with different Al layer thicknesses and total film thickness, respectively. The patterns only reveal the presence of diffraction peaks of face-centred cubic (fcc) Ni and Al, which indicates that all films are crystalline in the fcc phase. Although the multilayers were on the substrate, no peak of the substrate was observed in the patterns due to the amorphous structure of the substrate (data not shown). As seen in Fig. 2a, the GIXRD pattern of the Ni film has the (111) and (200) peaks of fcc Ni at $2\theta \approx 45.5°$and 52.0°, respectively , according to the JCPDS 88-2326. However, with the increase in Al layer thickness, the presence of strong fcc Al peaks co-existing with Ni peaks was observed. In Fig. 2b–d the Ni/Al films produced with Al layers thicknesses of 5.0, 10.0, 17.5 nm also show the Bragg reflections of (111), (200), (220) and (311) planes of the fcc phase for Al at $2\theta \approx 38.4°$, 44.7 °, 65.1° and 78.2°, respectively, according to the JCPDS 04-0787. As can be seen from Fig. 2, the intensity of the Al (111) peak at about 38° is gradually increased with increase in the Al layer thickness with the increase of Al content in the films. Besides, the peak formed at $2\theta \approx 45°$ in the GIXRD patterns of Ni/Al multilayers also exist in the GIXRD pattern of the Ni film, thus this peak is occurred from the reflections of the Ni (111) and as well as Al (200) planes. Therefore this peak is shown as Ni (111) + Al (200) in patterns of Ni/Al multilayers. These peaks were also observed in [18]. And, the (200) peak of Ni film at $2\theta \approx 52°$ in Fig. 2a disappeared in Ni/Al multilayer films with the increase of Al content in the films caused by the Al layer thickness. The peaks of Al (220) and Al (311) were not observed in the same study [18]. The crystallite sizes, t values of the highest peak of (111) plane in the patterns of the multilayers were calculated by the Scherrer Eqs. [19, 20]. The sizes of the (111) crystallites in Ni film were found to be ~ 7 nm. For Ni/Al multilayers, the t values of Al (111) plane

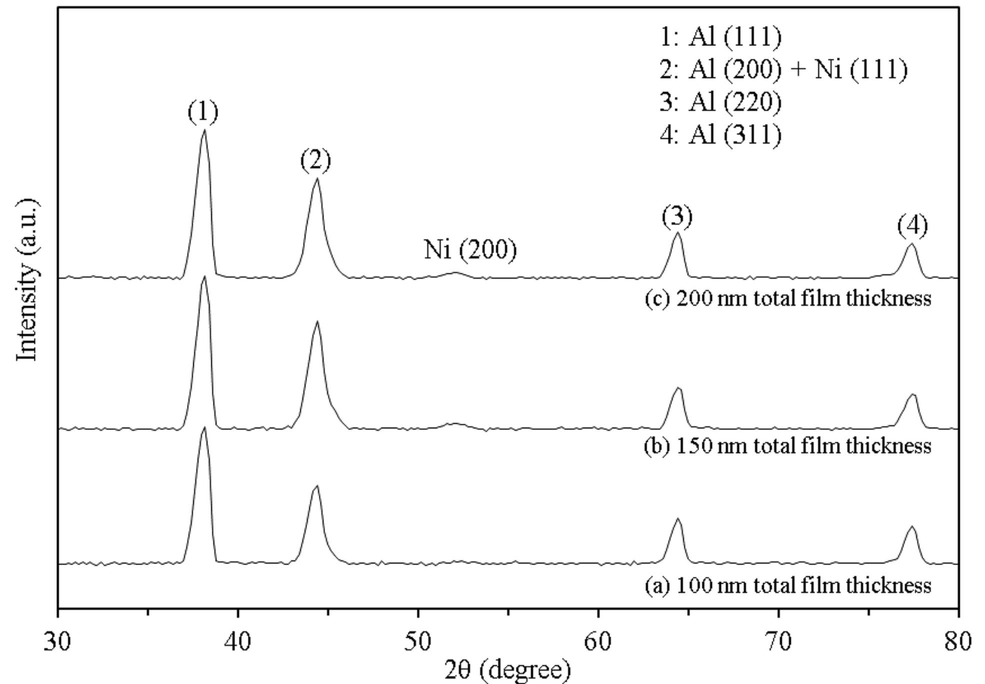

Fig. 3 The GIXRD patterns of the Ni/Al films produced with different total thicknesses

were obtained as ~ 10 nm for all films produced with different Al layer thicknesses. The ~ 7 nm crystallite size of (111) plane for Ni film slightly increased to ~ 10 nm for Ni/Al multilayer films produced with different Al layer thicknesses. The interplanar spacing, d values were calculated from Bragg formula [20] and given in Table 1. They are not much changed. Besides, the lattice constant, a value of the Ni film was calculated as 0.3508 nm from GIXRD data of all peaks, while the a values of Ni/Al multilayers were ~ 0.4092 nm which are higher than that of Ni film. The high Al content results an increase in the a values of the multilayers since the a values of bulk Ni and Al are 0.3524 and 0.4049 nm, respectively.

In the case of total film thickness, the GIXRD patterns of the films are shown in Fig. 3. The fcc (111) peak of Al is the highest peak for all of the multilayers. In Fig. 3, unlike the GIXRD patterns of the multilayers produced with different Al layer thicknesses, the peak belongs to the (200) plane of Ni content begun to appear at ~ 53° in the pattern of the film which has a total film thickness of 150 nm and the intensity of this peak increased when the total thickness was 200 nm. The crystallite size was found to be nearly same as ~ 8 nm irrespective of different total film thickness. The a values of the Ni/Al films deposited at different total thicknesses are between 0.4081 and 0.4086 nm as indicated in Table 1.

SEM images of the multilayers sputtered at different Al layer and total film thicknesses were given in Figs. 4 and 5, respectively. As seen in the images, the surface of the multilayer films has granular structure. And these granules are uniformly and closely distributed on the surface of the films. Besides, as seen in Fig. 4a, unlike the surface of multilayer films, the presence of a small number of clustered granules with sizes varying around 1–2 µm is also noticed on the surface of the Ni film. And these clustered granules were not formed when the multilayered structure forms in Fig. 4b–d. As can be seen from Fig. 4, all multilayers produced considering different Al layer thicknesses show quite similar morphologies. And, the multilayer surfaces were homogeneously covered with nanoscale granules with a diameter of ~ 100 nm. The results show the surface homogeneity of Ni/Al multilayers is larger than Ni thin film. For the film surfaces with different total film thicknesses in Fig. 5a–c, it is obvious that the size of the granules were almost similar for the total film thicknesses of 100 and 150 nm, but slightly increased for the total film thickness of 200 nm.

Hysteresis loops of Ni/Al multilayer thin films with different Al layer and total film thicknesses are plotted at ± 5 kOe as shown in Figs. 6 and 7 (loops at ± 300 Oe are shown in the inset), respectively. Magnetization studies indicate that all Ni/Al multilayer films are ferromagnetic in nature. As can be seen from Fig. 6, the saturation magnetization, M_s of 572 emu/cm^3 was

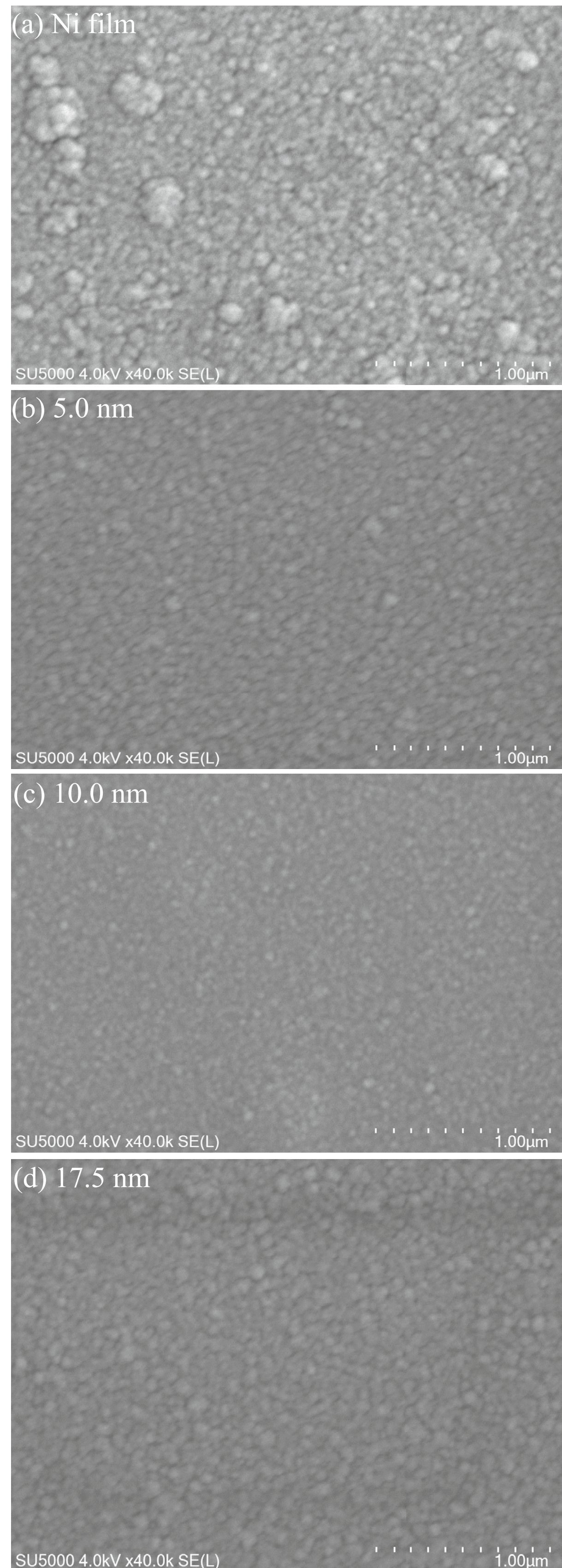

Fig. 4 SEM images of the **a** Ni film and Ni/Al multilayers produced with **b** 5.0, **c** 10.0 **d** and 17.5 nm thicknesses of the Al layers

achieved in the Ni film. When multilayered structures containing Al layers were formed the M_s value decreased. For Ni/Al multilayer films with Al layer thicknesses of 5.0, 10.0 and 17.5 nm, the M_s values were obtained as 441, 383 and 298 emu/cm^3, respectively. It is clearly seen in Fig. 6 that M_s decreases with increasing Al layer thickness due to the increase of Al content in the film. Since M_s depends on the type and percentage of the magnetic components, M_s values of the multilayers were consistent with the elemental analysis as seen in Table 1. Accordingly, the increase of Al content and the decrease of Ni content with increasing Al layer thickness caused a decrease in the M_s value. Magnetisation studies for the total film thickness showed a slight and gradual decrease of M_s from 450 to 427 emu/cm^3 with increasing total film thickness from 100 to 200 nm as seen in Fig. 7. This is expected since the Ni content of the multilayers decreases slightly from 60.4 to 55.5 at.% with the increasing total film thickness. The saturation magnetization of Ni/Al multilayer thin films were shown to be quite sensitive to the Al layer and total film thicknesses.

On the other hand, the coercivity, H_c values of the multilayers was ~ 39 Oe for different Al layer thickness. The H_c of the Ni film was obtained as 90 Oe and this value was found to be almost two times higher than the H_c of the multilayers, see Table 1. This can be attributed to the clustered granules of different sizes seen in the SEM image of Ni film. Since, H_c can be affected by the structural properties especially the change in the microstructure such as the size of surface grains [21]. In addition, the similar SEM images of the Ni/Al multilayers may cause that the H_c values are between 38 and 52 Oe according to the different total film thicknesses. In both cases, the H_c values are between the limits of soft (12.5 Oe) and hard (125 Oe) magnetic properties [2].

4 Conclusions

Ni/Al multilayer films were produced on acrylic acetate substrate by a dual magnetron sputtering. The effects of different Al layer thicknesses and total film thickness on the structural and related magnetic

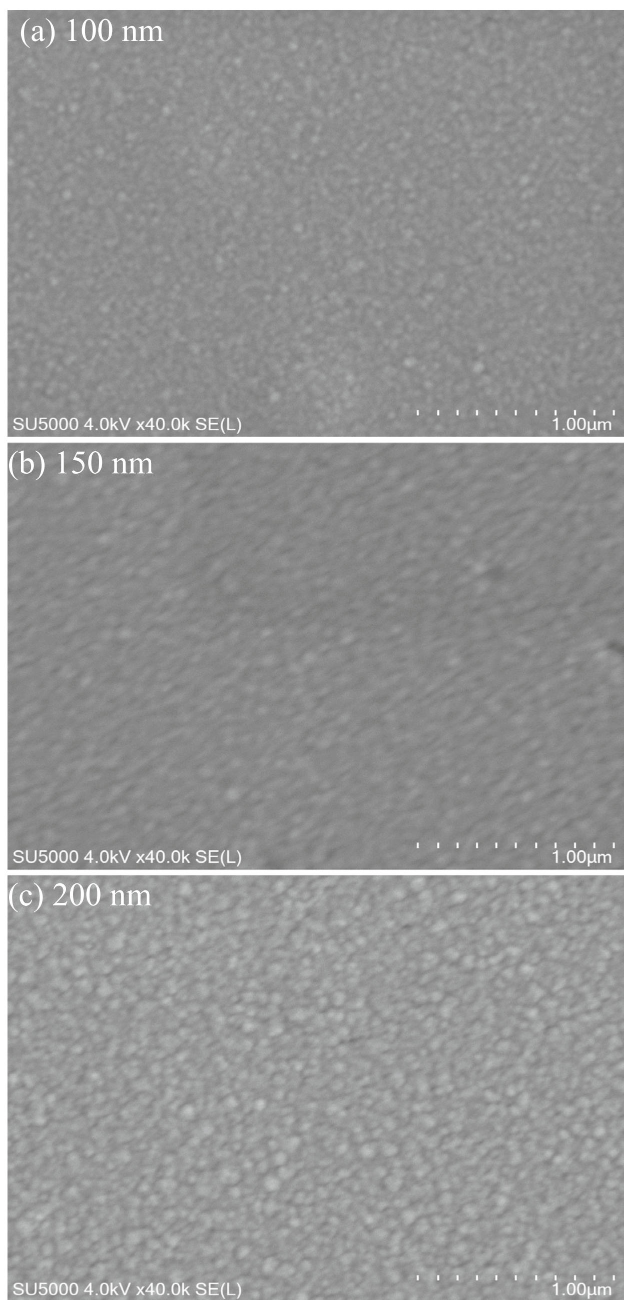

Fig. 5 The SEM images of the Ni/Al multilayers films with **a** 100, **b** 150 and **c** 200 nm total thicknesses

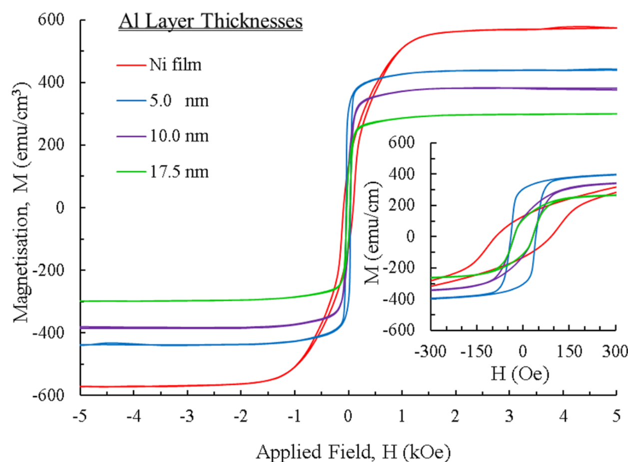

Fig. 6 Hysteresis loops of Ni film and Ni/Al multilayers produced with different thicknesses of Al layers plotted at ±5 kOe (Inset presents the loops at ±300 Oe)

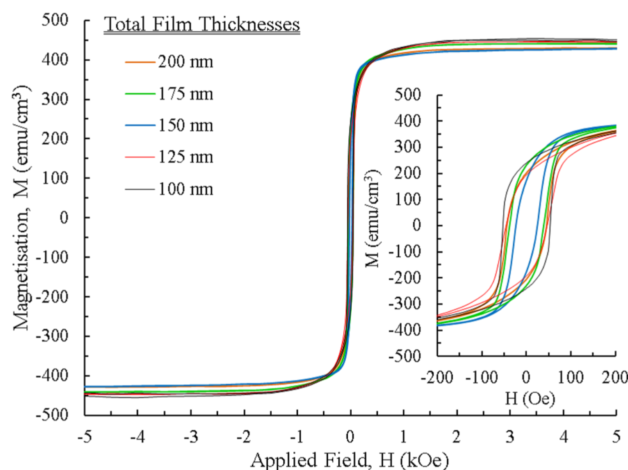

Fig. 7 Hysteresis loops of Ni/Al multilayers produced with different total thicknesses plotted at ±5 kOe (Inset presents the loops at ±200 Oe)

properties of Ni/Al multilayer thin films were investigated. The Ni film was also produced and compared with the properties of Ni/Al multilayers. Composition analysis showed that with increasing Al layer thickness, the Al content of the multilayers increased while the Ni content decreased. Besides, the Ni and Al content of the multilayers varied slightly with the total film thickness. GIXRD analysis indicated that all multilayer films presence the fcc phase and the Al (111) peak intensity increased with the increase of Al content in the films caused by the Al layer thickness. The morphological analysis showed that Ni/Al multilayer films have uniformly distributed granular surfaces. On the other hand, the surface of the Ni film has clustered granules with the size of ~ 1–2 µm. None of these clustered granules were formed on the surface of the Ni/Al multilayers. With the increase of the total thickness, the size of the granules increased slightly. For the magnetic analysis, Al layer thickness was found to have a significant impact on the saturation magnetisation of the Ni/Al multilayer films. The M_s of the Ni film was obtained as 572 emu/cm^3.

And, the gradually decrease in M_s of the Ni/Al multilayers from 441 to 298 emu/cm^3 can be explained by the increase in Al content and the decrease in Ni content as the Al layer thickness increases from 5.0 to 17.5 nm. And, a slight decrease in M_s value was observed with increasing total film thickness. And, the H_c of the Ni film was detected as 90 Oe. The H_c value of the multilayers for different Al layer thickness was ~ 39 Oe which is softer than the Ni film. The lack of clustered granules on the multilayer surfaces may result in the decrease of H_c value. It is observed that the parameters of Al layer thickness and total film thickness helped to understand the structural and related magnetic properties of Ni/Al multilayer films suitable for wide range of magnetic applications as microelectronic devices.

Author contributions

N. Kaplan produced the films and prepared the table and figures and also wrote the draft of article. H. Kuru wrote the article and take and analysis the VSM measurements. H. Köçkar planned and directed the study and also contributed to the interpretation of the results.

Funding

Open access funding provided by the Scientific and Technological Research Council of Türkiye (TÜBİTAK). This study was supported by Balikesir University, Turkey under Research Grant no. BAP 2022/068. The authors thank the State Planning Organization, Turkiye under grant no 2005K120170 for Physical Vapor Deposition system and Vibrating Sample Magnetometer systems. The authors are grateful to Karamanoglu Mehmetbey University, BILTEM, Turkiye for SEM, EDX and XRD measurements. Nadir Kaplan also privately thanks the Scientific and Technological Research Council of Turkey (TÜBİTAK), 2211-C National Scholarship Programme for Ph.D. study.

Data availability

The authors declare that they have the data availability statement in their manuscript.

Declarations

Conflict of interest The authors declare that they have no conflict of interest.

Open Access This article is licensed under a Creative Commons Attribution 4.0 International License, which permits use, sharing, adaptation, distribution and reproduction in any medium or format, as long as you give appropriate credit to the original author(s) and the source, provide a link to the Creative Commons licence, and indicate if changes were made. The images or other third party material in this article are included in the article's Creative Commons licence, unless indicated otherwise in a credit line to the material. If material is not included in the article's Creative Commons licence and your intended use is not permitted by statutory regulation or exceeds the permitted use, you will need to obtain permission directly from the copyright holder. To view a copy of this licence, visit http://creativecommons.org/licenses/by/4.0/.

References

1. Y. Cao, J. Zhang, Y. Liang, F. Yu, T. Sun, Appl. Surf. Sci. **257**, 847 (2010)
2. D. Jiles, *Introduction to magnetism and magnetic materials* (Chapman and Hall, London, 1996)
3. P. Ripka, Meas. Sci. Technol. **13**, 645 (2002)
4. H. Shen, B. Gao, S. Pan, L. Liu, G. Yang, J. Magn. Magn. Mater. **587**, 171310 (2023)
5. S. Çölmekçi, A. Karpuz, H. Köçkar, Thin Solid Films. **727**, 138661 (2021)
6. Y. Wang, Z. Xing, Y. Qiao, H. Jiang, X. Yu, F. Ye, Y. Li, L. Wang, B. Liu, J. Alloys Compd. **789**, 887 (2019)
7. B. Borca, C. Bartha, Coatings. **12**, 1138 (2022)
8. J.B. Yi, Y.Z. Zhou, J. Ding, G.M. Chow, Z.L. Dong, T. White, X. Gao, A.T.S. Wee, X.J. Yu, J. Magn. Magn. Mater. (2004). https://doi.org/10.1016/j.jmmm.2004.06.052
9. M. Kumar, Mater. Res. Express. **6**, 126408 (2019)
10. K.S. Sathish, A. Sharma, R.G. Mohan, S. Suwas, J. Alloys Compd. **695**, 1020 (2017)
11. M. Kumar, R. Mitra, Surf. Coat. Technol. **251**, 239 (2014)
12. B.C. Kang, Hee, H.Y. Kim, O.Y. Kwon, Soon, S.H. Hong, Scripta Mater. **57**, 703 (2007)

13. J. Noro, A.S. Ramos, M.T. Vieira, Intermetallics. **16**, 1061 (2008)
14. S. Simões, F. Viana, A.S. Ramos, M.T. Vieira, M.F. Vieira, Intermetallics. **19**, 350 (2011)
15. S.W. Kuk, H.J. Ryu, J. Yu, J. Alloys Compd. **589**, 455 (2014)
16. K. Jaekel, Y.H. Sauni Camposano, S. Matthes, M. Glaser, P. Schaaf, J.P. Bergmann, J. Müller, H. Bartsch, J. Mater. Sci. **58**, 12811 (2023)
17. A. Karpuz, H. Köçkar, S. Çölmekçi, Acta Phys. Pol. A **134**, 1180 (2018)
18. M. Swain, S. Singh, S. Basu, D. Bhattacharya, R.B. Tokas, M. Gupta, J. Alloys Compd. **631**, 46 (2015)
19. R.A. Mahesh, R. Jayaganthan, S. Prakasha, V. Chawla, R. Chandra, Mater. Chem. Phys. **114**, 629 (2009)
20. B. Cullity, *Elements of X-ray diffraction* (Addison-Wesley, Massachusets, 1978)
21. A. Karpuz, H. Kockar, M. Alper, Appl. Surf. Sci. **358**, 605 (2015)

Publisher's Note Springer Nature remains neutral with regard to jurisdictional claims in published maps and institutional affiliations.